Nuclear Inst. and Methods in Physics Research, A 887 (2018) 114–121

Contents lists available at ScienceDirect

Nuclear Inst. and Methods in Physics Research, A

journal homepage: www.elsevier.com/locate/nima

Feasibility study of a cyclotron complex for hadron therapy

V. Smirnov *, S. Vorozhtsov

Joint Institute for Nuclear Research, Dubna, Russia

ARTICLE INFO

Keywords:
Cyclotron
Hadron therapy
Superconductivity
Computer simulation
Beam dynamics
Electromagnetic fields

ABSTRACT

An accelerator complex for hadron therapy based on a chain of cyclotrons is under development at JINR (Dubna, Russia), and the corresponding conceptual design is under preparation. The complex mainly consists of two superconducting cyclotrons. The first accelerator is a compact cyclotron used as an injector to the main accelerator, which is a six-fold separated sector machine. The facility is intended for generation of protons and carbon beams. The H_2^+ and $^{12}C^{6+}$ ions from the corresponding ECR ion sources are accelerated in the injector-cyclotron up to the output energy of 70 MeV/u. Then, the H_2^+ ions are extracted from the injector by a stripping foil, and the resulting proton beam with the energy of 70 MeV is used for medical purposes. After acceleration in the main cyclotron, the carbon beam can be either used directly for therapy or introduced to the main cyclotron for obtaining the final energy of 400 MeV/u. The basic requirements to the project are the following: compliance to medical requirements, compact size, feasible design, and high reliability of all systems of the complex. The advantages of the dual cyclotron design can help reaching these goals. The initial calculations show that this design is technically feasible with acceptable beam dynamics. The accelerator complex with a relatively compact size can be a good solution for medical applications. The basic parameters of the facility and detailed investigation of the magnetic system and beam dynamics are described.

1. Introduction

Development of accelerators for producing carbon beams with the energy of 400–450 MeV/u for hadron therapy appears to be an increasingly important issue nowadays. The existing facilities for this purpose are mainly based on synchrotrons. It seems interesting to use isochronous cyclotrons instead, as is the case in proton therapy. However, the so far developed designs of compact superconducting cyclotrons have some disadvantages in addition to their advantages [1]. An alternative solution can be a facility based on a separated sector cyclotron justified in [2]. According to this reference, an attractive characteristic of this dual cyclotron solution is the option of a two-phase realization, since the high-energy carbon option can be added later, but in the first phase and already from the start of the project "low-energy" carbon-based particle therapy can be employed, together with the full spectrum of proton energies using acceleration of H_2^+ ions in the same machine. The design of this facility should comply with a number of conditions. First, the size and weight of the main accelerator must be as small as possible, which makes it expedient to use the highest possible magnetic field. Second, the injection energy should be low enough for the injector-cyclotron to be of reasonable size. Third, the magnetic system design should be feasible, that is, the parameters of the superconducting coil (engineering current density, acting forces, etc.) should be adequate and the space between the sectors should be large enough to accommodate accelerating elements, beam injection system, etc. A separate task is to develop the magnet of the main machine such that it will maintain isochronism of the magnetic field and particle focusing along with a minimum number of resonance crossings by the beam during acceleration. Our proposal, which meets all the above-mentioned requirements, is an acceleration setup (Fig. 1) consisting of a compact injector-cyclotron (K280) and the main separated-sector cyclotron (K1600). Both cyclotrons are superconducting.

The proposed acceleration cascade having an external size of about 15 m is smaller than the synchrotron-based facilities for hadron therapy and has typical advantages of a cyclotron. Besides, building a synchrotron does not allow the phased approach. For comparison, below are the sizes of some similar facilities based on synchrotrons:

- HIT (Heidelberg, Germany) [3], final beam energy 430 MeV/u, size (with injector) ~40 m;
- CNAO (Pavia, Italy) [4], final beam energy 400 MeV/u, size (with injector) ~24 m;

* Corresponding author.
E-mail address: vsmirnov@jinr.ru (V. Smirnov).

https://doi.org/10.1016/j.nima.2018.01.046
Received 18 December 2017; Received in revised form 9 January 2018; Accepted 15 January 2018
0168-9002/

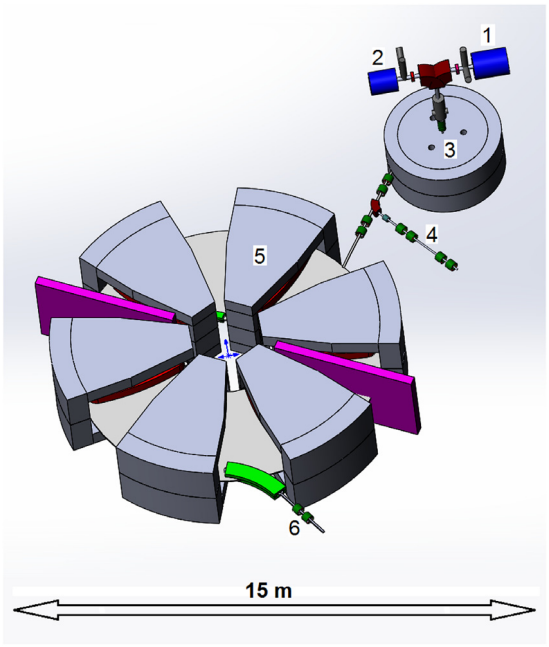

Fig. 1. Acceleration complex layout: 1-$^{12}C^{6+}$ ECR, 2-H_2^+ ECR, 3-K280, 4-medium energy beam transport line (proton and carbon 70 MeV/u), 5-K1600, 6-high energy beam transport line (carbon 400 MeV/u).

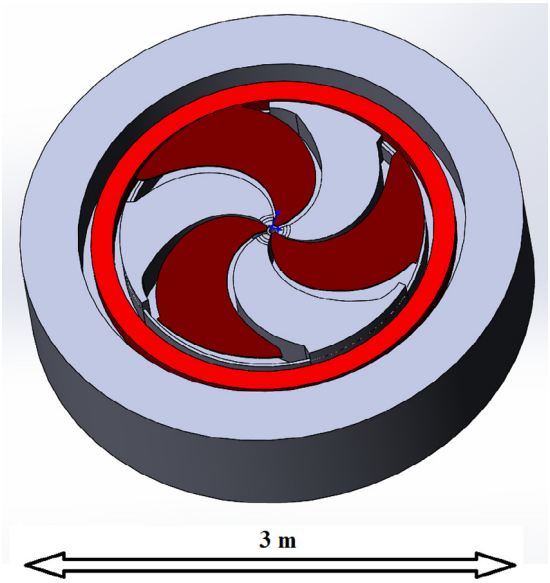

Fig. 2. K280 layout.

- HIMM (Lanzhou, China) [5], final beam energy 400 MeV/u, size (with injector) ~27 m.

The preliminary results on the project are presented in [6] and [7]. The latest developments in the facility design are described in the following sections.

2. The injector-cyclotron

The carbon injection energy to K1600 is chosen to be 70 MeV/u because the K280 with this final energy can be also used as a stand-by facility for medical applications having in mind a possibility of H_2^+ ions acceleration in addition to carbon ions. In the H_2^+ regime magnetic field of the cyclotron should be slightly corrected by dedicated trim coils foreseen in the accelerator design similar to that described in [8]. A spiral inflector, which will be used in the central region of the cyclotron for beam injection, has the same structure for both carbon and hydrogen ions, since their charge-to-mass ratios are almost identical. Subsequent stripping of H_2^+ ions allows obtaining protons with energy suitable for treating eye melanomas and skin cancer, or producing radioisotopes. A compact superconducting cyclotron seems to be the most optimal option for this machine. The magnetic rigidity of 70-MeV/u $^{12}C^{6+}$ ions is about that of 250-MeV protons. So, the injector design can be based on the proven technology that is used in modern accelerator setups [9–12]. Some technical solutions of these machines are applicable to the K280. The use of external ion sources limits the central magnetic field to a maximum of 3.0 T due to injection through the spiral inflector. Another constraint comes from the necessity of having the same acceleration frequency in the injector and in the K1600. This also influences the choice of the central magnetic field in the K280. Considering the above said, two variants of the injector design are initially investigated: a four-fold magnetic structure with the 1.98 T central field and a three-fold magnet with the 2.64 T central field. The central field level is defined by the choice of the RF harmonic mode of the accelerator – four or three – to provide the required frequency of the acceleration system in accordance with the K1600 acceleration frequency (synchronization). Both cases imply placement of spiral dees in all valleys of the magnetic structure to ensure maximal energy gain per turn. The four-fold structure has the highest energy gain per turn leading to more efficient particle extraction from the cyclotron vacuum chamber. An advantage of the three-fold structure is a higher magnetic field that allows a more compact and lighter magnet. This is why the three-fold option was selected as a baseline for the injector-cyclotron (Fig. 2). The field index has a moderate value at the final radius, and there is no problem with obtaining a sufficient magnetic flutter for the axial focusing of accelerated particles. This permits a sufficiently large axial air gap between the spiral sectors for the extraction system elements to be placed in this gap (Table 1). Considering the above said, the expected beam extraction efficiency of 80% can be achieved rather easily. The required spirality of the magnetic sectors at the final radius is below 55° to provide the axial betatron frequency near 0.3. The radial betatron frequency is below 1.2 at the selected final energy of the beam. This prevents crossing a dangerous resonance $2Q_r = 3$, which normally limits the final energy in a cyclotron with the three-fold magnetic structure.

The SUPERNANOGAN 14.5 GHz ECR PANTECHNIK [13] based on permanent magnets is considered as the $^{12}C^{6+}$ ion source for the cyclotron. The available intensity of the ions from this source is 2.5 μA at the maximal extraction voltage of 30 kV. The company can deliver the unit together with the beam transport system including the Einzel lens, the double focusing dipole, two steerers, slits, the beam profiler, the Faraday-cup, and the complete gas system. Similar to the carbon beam, H_2^+ ions can also be obtained from an ECR ion source.

3. Medium-energy beam transport

The purpose of the medium-energy beam transport (MEBT) line is to deliver the beam extracted from the K280 to the K1600 with the required beam quality. Currently, the system is at an early design stage, and its structure details are not fully defined yet. In the initial assumption, several duplets of magnetic quadruples, magnetic steerers, and a beam diagnostics system are considered. In the case of using beams, accelerated in the K280, directly for medical purpose, the corresponding bending magnet is switched on to divert ions in the dedicated beam line (see Fig. 1). The final decision on the MEBT structure will be taken after detailed simulation of the beam dynamics in the K280 and in the MEBT. For example, additional bending magnets could be installed in the MEBT to take into account the final relative position of the cyclotrons in the cascade.

Table 1
Basic parameters of the cyclotrons.

	K280	K1600
Cyclotron type	Compact, isochronous	Separated sectors, isochronous
Ion type	H_2^+,$^{12}C^{6+}$	$^{12}C^{6+}$
Final beam energy	70 MeV/u	400 MeV/u
Final beam intensity: carbon/proton	600–800 nA/250 μA	100 nA
Final beam emittances	10–20 π mm mrad	<20 π mm mrad
Magnetic system	3 spiral sectors	6 radial sectors
Average magnetic field: injection/extraction	2.6 T/2.9 T	1.3 T/1.8 T
Hill magnetic field: injection/extraction	2.6 T/3.7 T	3.5 T/5.1 T
Acceleration system	3 spiral cavities	2 single-gap cavities
Acceleration voltage	90 kV	450 kV
Acceleration frequency	60.77 MHz	60.77 MHz
Acceleration mode	3	6
Average radius: injection/extraction	15 mm/870 mm	1730 mm/3370 mm
Dimensions: diameter/height	3000 mm/1400 mm	9000 mm/2200 mm
Total weight (sectors + coils)	~70 t	~520 t

4. The main cyclotron

Parameters of the K1600 are very important for defining overall characteristics of the whole accelerator complex. So, to compete with synchrotrons of similar application, its size should be less than 10 m. The weight should be less than 600–700 t, which is characteristic of the compact cyclotron with the same final energy [14]. The required parameters can be reached by using a superconducting magnetic system with the field about 5 T. To provide sufficient final beam intensity, the partial efficiency of the beam injection, acceleration, and extraction from the cyclotron should be no less than 80%–90%. The basic parameters of the K1600 to meet the requirements formulated above are presented in Table 1.

4.1. Magnetic system

A possibility of creating a cyclotron magnetic system on the basis of superconducting sector magnets is discussed in [15]. In this publication various options of possible configurations of the magnetic system of the K1600 depending on the field level are considered. Dependence of the characteristics of the magnetic field on the location and form of the superconducting coils is also analyzed. The choice of the most optimal structure is made. All the magnetic field calculations were performed on a three-dimensional basis using the TOSCA\Opera3D code.

A substantial difference between the injection and extraction energies in the K1600 leads to a considerable decrease in the magnetic field flutter from the initial to the final radius, which makes the working point to cross dangerous resonances. To obtain a higher flutter value at the final radius, the axial gap between the upper and lower coils should be smaller in this region. This coil arrangement leads to a smaller average magnetic field at the injection radii. A suitable enlargement of the azimuthal width of the sectors can correct this undesired change of the average files there. On the other hand, there should be sufficient room between the neighboring sectors for accommodating the coil cryostats and acceleration system structure. According to the existing literature on the subject, the engineering current density is allowed below 150 A/mm^2 (critical value). Obviously, the real operational value should be noticeably smaller, namely, at a level of 50–70 A/mm^2. In this case, the following practical requirements were assumed when designing the magnet: (a) the free space assigned for installation of the coil cryostats should be more than 70 mm; (b) the axial gap between the coils should be more than 120 mm; (c) no concave sectors of the coil are allowed.

From dedicated calculations it was found that for compliance with the above requirements, the central magnetic field, governing the particle circulation frequency, should be less than 1.3 T. In this case, the final radius of 400 MeV/u ions will be 337 cm, making the external diameter of the cyclotron about 9 m (Fig. 3). A tendency to keep the axial betatron oscillation nearly invariable vs. the radius requires some enlargement of field flutter at medium radii by making the coil more convex there. This shape also allows avoiding additional problems with forces acting on the coil.

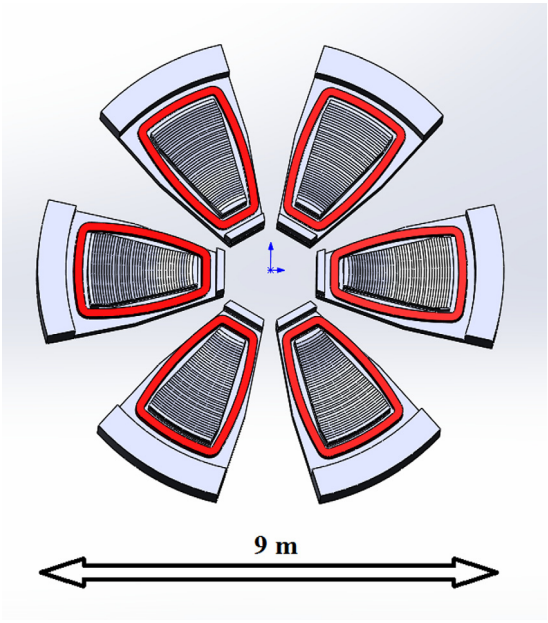

Fig. 3. Magnetic system of the K1600.

The yoke of the sector externally measures 3.6 × 2.7 × 2.2 m^3. The sector weighs 85 t (coil 5 t). The operational engineering current density in the superconducting coil is 62 A/mm^2, and its cross section is 160 × 260 mm^2. The coils are tilted with respect to the median plane at angles of ±3.5°. Axial profiling of the poles (Fig. 4) is used to shape the isochronous field. The air gap between the poles is minimal in the injection and extraction regions, 82 and 78 mm respectively. At the middle radii the gap reaches 390 mm. The magnetic induction in the region of the coil is as high as 5.3 T. The maximum field is 5 T in the hills, 2.7 T in the yoke, 5 T in the pole, and −1.2 T in the valley.

The superconducting cyclotrons applied for hadron therapy should be operated at minimal cryogenic infrastructure at use of so called cryocoolers. The fringe field at the cryocooler head should be less than 0.05 T. At the present design stage it is assumed that the thicknesses of the horizontal and vertical yokes of the sector magnet are only 400 and 550 mm respectively. The calculations show that even without dedicated magnetic shielding of the space between the sector magnets, the fringe field is about 0.05 T on 2.2 m distance from the yoke. So, the cryocoolers can be located at the indicated position. But they can be deployed closer to the cyclotron center by reducing the fringe field outside the magnet yoke where also the beam transport lines and other

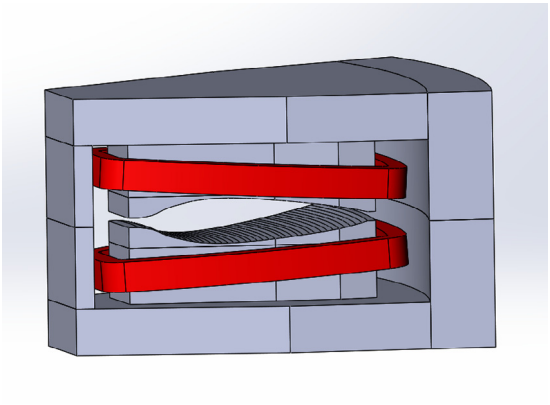

Fig. 4. Magnet sector.

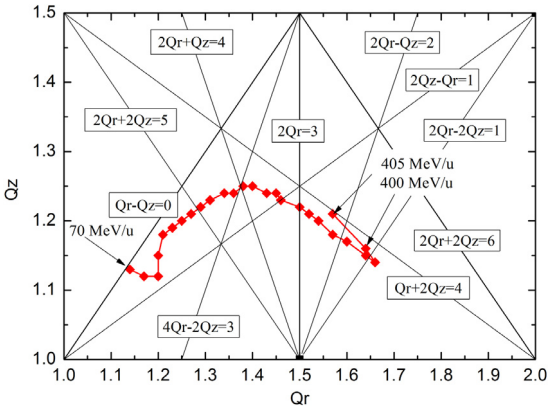

Fig. 5. Tune diagram.

structures should be installed. This field reduction can be ensured by the corresponding increasing of the sector yoke thickness.

Varying the azimuthal size of the sectors and the position of the coils, we can find the structure characterized by a flutter increasing with radius and a minimal change of the axial betatron frequency Qz (Fig. 5) while the average magnetic field is approximately isochronous. Variation of the azimuthal size of the coil leads to a shift of the axial betatron frequency over the whole range of the acceleration radii preventing the working point from crossing dangerous resonances ($Qz = 1, 2Qz = 3, Qr - Qz = 0$). Unfortunately, crossing of some resonances of the third and fourth orders cannot be avoided. But some variation of the magnetic system parameters (flutter, spirality) could probably help for example in $2Qr - 2Qz = 1$ resonance case. Also, our previous experience and existing practice with other machines show that this is not an issue with relatively small tolerances on the corresponding magnetic harmonics imposed. Nevertheless, there is a corresponding plan for investigation of the impact of those resonances on the beam stability in near future.

Isochronization of the obtained field distribution can be performed by following a procedure described below. The approximate radial dependence of the isochronous field has the form

$$B(r) = b \cdot \left[1 - \left(\frac{r}{a}\right)^2\right]^{-1/2}, \quad (1)$$

$$a = c/\omega_0, \quad b = m \cdot \omega_0/q,$$

where m is the ion mass, q is the ion charge, and ω_0 is the particle circulation frequency. After shaping the field in accordance with (1), a better approximation to the isochronous curve can be obtained following Gordon's algorithm [16] based on magnetic field parameters (flutter, maximal spiral angle) calculated at the initial step above. For the eventually found field map, a set of static equilibrium orbits can be calculated by a particle tracing code in a range of particle energies. Then, the magnetic field at the closed orbit gets scaled by a ratio of the cyclotron over the orbital frequencies making the field map closer to the isochronous one. The procedure applies to all orbits in the acceleration range. Repeating the procedure two or three times, one can obtain the convergence with the particle RF phase deviation no more than ± 10°. Normally, the field variation is within ±10 Gs in this case.

4.2. Acceleration system

The particle acceleration is provided by two single-gap cavities located in the valleys of the magnetic structure. The acceleration voltage amplitude of 450 kV at each cavity does not look unrealistic, considering, for example, a similar acceleration structure with 500–650 kV at the RIKEN RIBF complex [17]. In addition, in the further design study the requirements to the acceleration system could probably be eased, including reduction of the acceleration voltage. Also, increase of the turn number due to lower voltage does not look like a critical limiting factor. Now the minimal space between the coil cryostats available for deployment of the resonators is 350 mm. The selected acceleration frequency is more or less common to what is normally used in modern cyclotrons. All the said above leads to a conclusion that the design and construction of the RF system will be rather feasible. At this stage of the beam dynamics simulations the energy gain per acceleration gap was specified analytically in accordance with the acceleration voltage and the particle RF phase. In this case, the central particle makes ~760 revolutions to reach the final energy.

4.3. Injection system

The beam injection system is one of the critical issues in the K1600 design. It requires non-negligible time for formulation of a suitable system structure and assessment of its optimal functionality from point of view of beam dynamics. For example, at the initial stage of the consideration a superconducting ironless septum magnet was conceived to bend the beam in the direct vicinity to the internal cyclotron orbits [7]. But such critical factors as a rather large magnetic field along with insufficient space allocated for the coil cryostat demanded redesign of the unit. As a result of the tedious process, the injection system was assembled from three superconducting bending magnets (IBM1-IBM3), a passive magnetic channel (IMC), and two electrostatic inflectors (ESI1 and ESI2s), see Fig. 6. The required central fields in the bending magnets are −1.5, 1.6, and 1.2 T with the engineering current density ranging from 50 to 130 A/mm^2. The field drop in the magnetic channel is 0.2 T. The structure of the injection system magnets was designed such as to provide increasing or decreasing magnetic fields across the injected beam path allowing compensation of the negative impact of the sector magnet field on the injected beam quality. The transverse field gradients of the magnets are −8, −6, 4, and 3 T/m.

At injection the axial gap between the upper and lower sector coils is ~600 mm allowing insertion of the first and second injection magnets in between. In addition, the axial gap between the poles of the sector magnet permits installing the third injection magnet at the required location, see Fig. 6.

Calculation of the magnetic field in the injection system magnet is performed with allowance for the sector field effect that reached ~3.7 T at their locations. Obviously, the sector field changes the magnetization of the injection magnets, which essentially modifies their magnetic field. For some magnets, even the induction direction changes its sign in the return yoke. Due to lack of space the construction of the IMB1 and IMB2 requires that their coil cryostats also contain return yokes (see for example Fig. 7). Each of these injection magnets weighs about 150 kg. The "warm" part of the IMB1 and IMB2 consists of the pole and the vacuum chamber. Such a construction allows optimal fixation of the

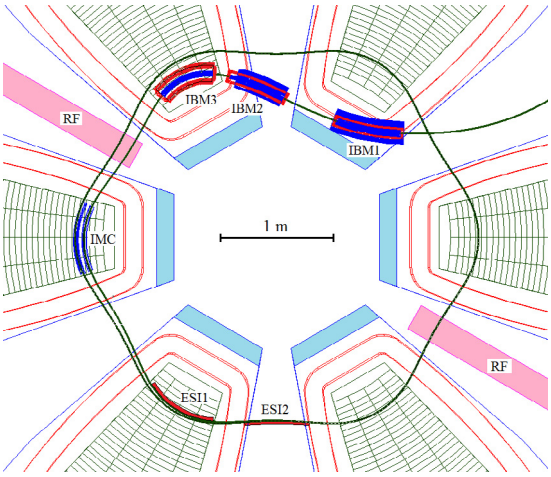

Fig. 6. Injection system of the K1600: IBM1-IBM3 are the injection bending magnets, IMC is the injection magnetic channel, ESI1 and ESI2 are the electrostatic inflectors.

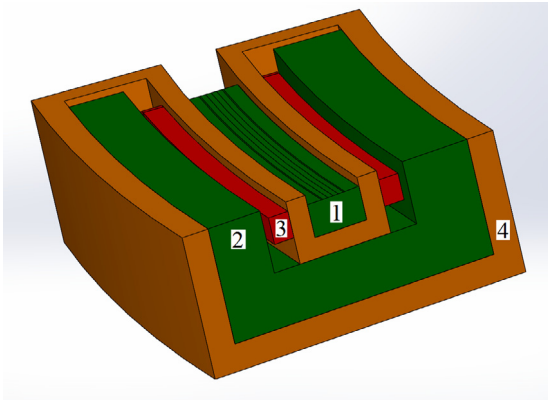

Fig. 7. Structure of the first injection bending magnet: 1-warm pole, 2-cold yoke, 3-superconducting coil, 4-cryostat.

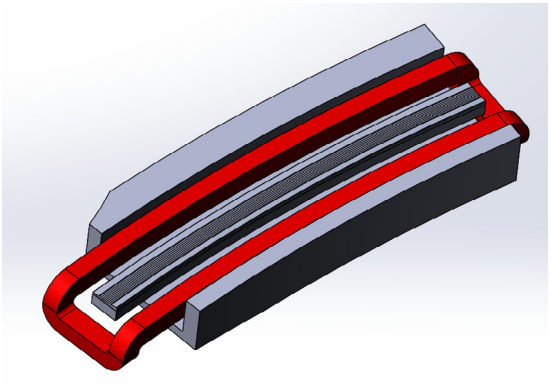

Fig. 8. Optimized structure of the second injection magnet.

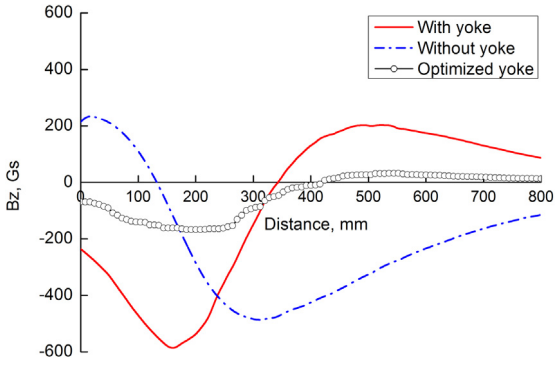

Fig. 9. Magnetic field perturbation from the second injection magnet in the first internal beam orbit.

coils to withstand applied ponderomotive forces. The cold and warm parts of the magnets are separated by a 15-mm gap to provide proper isolation between them. Estimation of the Lorenz forces, acting on the parts of the magnet coils, shows that they are no more than 450 kgf in the radial direction and 520 kgf in the axial direction.

When designing the injection magnets, the focus was not only on their required field contribution but also on suppression of the main field perturbation by the magnets at the position of the initial orbits of the beam. To this end, the structure of the magnets was carefully optimized. As a result, the perturbation by the first magnet at the initial orbits was no more than 200 Gs.

On the contrary, the corresponding perturbation from the second magnet for the coil engineering current density of 88 A/mm^2, is rather large, reaching ~600 Gs for the initial magnet design. Moreover, since the magnet is situated not only in the valley but also in the hill of the cyclotron magnetic system, the sign of the perturbation changes depends on the magnet position. So, it is problematic to use simple shimming plates for suppression of the perturbation in the initial orbits. In this sense, the analysis of the partial contribution to the field perturbation of the magnet yoke and coil can probably help. For example, it was shown that the contributions of the return yoke and the coil are of opposite sign in the valley and of like sign in the hill region of the sector magnet. So, the perturbation from IMB2 in the valley can be compensated by a suitable shape of the return yoke with simultaneous variation of the coil parameters. As for the perturbation in the hill, it can be suppressed, for example, by removal of the IBM2 return yoke in this region (Fig. 8). Eventually, it became possible to reduce the field perturbation in the initial orbits down to ~180 Gs (Fig. 9). Further suppression of the field perturbation can be obtained by installation of shimming plates into the cyclotron sector gap near the region of interest. In addition, similar compensating plates should be installed at the opposite side of the magnet to eliminate the 1st magnetic harmonic from the shimming plates. In the above considerations, the engineering current density in the coil of IBM2 was 115 A/mm^2.

As was mentioned above, the third injection magnet is located in the gap between the poles of the sector magnet. The direction of its field coincides with the direction of the sector magnet field. The cyclotron field itself is so large that the resulting magnetic induction retains its direction in the return yoke of IBM3. This way, the contribution of the IBM3 return yoke adds to the contribution of its coil it the initial beam orbits, leading to rather large perturbation of 2.3 kGs. To mitigate this negative effect, it is sufficient to remove the return yoke of the injection magnet. This reduces the perturbation by a factor of 3, i.e. to ~ 800 Gs in the beam circulation zone. An additional winding around the IBM3 (Fig. 10) with the current opposite to the IBM3 current, permits further reduction of the perturbation by a factor of 4, i.e., to ~230 Gs (Fig. 11).

The space occupied by the IBM3 return yoke according to the initial design can be used for enforcement of the magnet cryostat and, more generally, for simplification of the magnet construction. The disadvantage of the injection magnet without the return yoke is its smaller effective length. The field of the third injection magnet along the beam path gets higher due to additional magnetization of its poles by the sector magnet permitting acceptable current densities for its main coil (~100 A/mm^2) and correction coil (~150 A/mm^2). The ponderomotive forces acting on parts of the magnet coils are the highest compared to that for other injection units due to the fact that the IBM3 sits in the gap of the sector magnet with a relatively large magnetic field there.

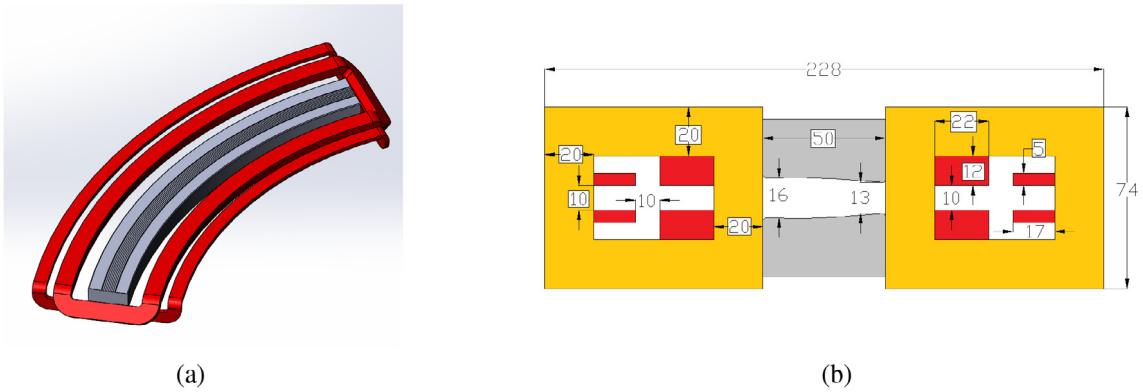

Fig. 10. The third injection magnet (a) and its cryostat (yellow) enclosing the coils (b). (For interpretation of the references to color in this figure legend, the reader is referred to the web version of this article.)

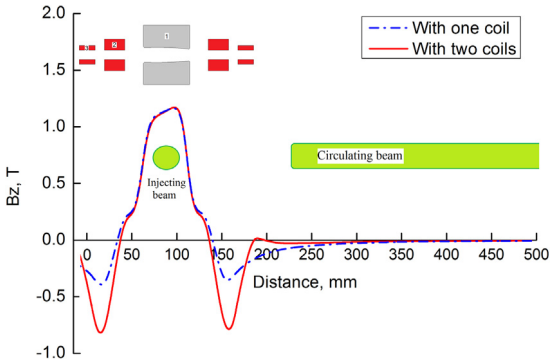

Fig. 11. Magnetic field contribution of the IBM3 with and without the correction coil: 1-poles, 2-main coil, 3-correction coil.

Fig. 12. Passive septum magnet nearest to the circulating beam.

For example, the characteristic radial force and the axial force in this magnet reach 450 kgf and 530 kgf respectively. The magnetic channel (IMC) with the septum 5 mm thick is the closest to the inner circulating beam. When optimizing the injection system structure as a whole, it was possible to come to the situation that the required field drop in the channel was 0.2 T. This permits construction of the channel as a passive septum magnet, i.e., without any coils in it (Fig. 12). The septum thickness is 5 mm in the magnet. The shimming plates located above and below the cyclotron inner orbits reduce the perturbation field of the magnet down to 200 Gs.

One of the electrostatic inflectors of 670 mm long is located between the magnetic sectors; another inflector of 560 mm long is installed in the valley. The aperture of the inflectors is 10 mm with the septum thickness increasing from 0.2 to 0.5 mm along its length. The strength of the electric field of the electrostatic inflectors is 80–90 kV/cm with slight variation for beam centering.

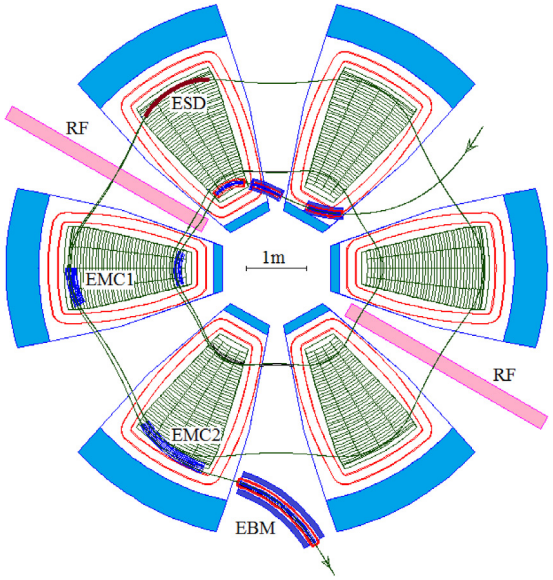

Fig. 13. Extraction system of the K1600: ESD is the electrostatic deflector, EMC1 and EMC2 are the extraction magnetic channels, and EBM is the extraction bending magnet.

4.4. Extraction system

The system for beam extraction from the K1600 consists of an electrostatic deflector (ESD), two passive septum magnetic channels (EMCs), and a bending magnet (EBM) (Fig. 13). The electrostatic deflector with its nominal field strength of 100 kV/cm is installed in the axial gap of the sector magnet. Its length of 130 mm allows its subdivision into several independently controlled parts to better fit to the extracted beam trajectory. The field drop of the passive magnetic channels is 0.25 T at the central line with their structure being analogous to the injection magnetic channel IMC. The required transverse magnetic gradients in the channels are 5 T/m and 15 T/m, which ensures minimization of the beam envelope of the extracted beam. The septum thickness in the channels is 5 mm and 8 mm respectively. The final element of the extraction system, IBM, has a 2.5-T flat field that implies a superconducting coil for the magnet excitation with the current density of ~100 A/mm^2. The coil is immersed into the magnet cryostat. To minimize the perturbation field from the magnet in the inner cyclotron

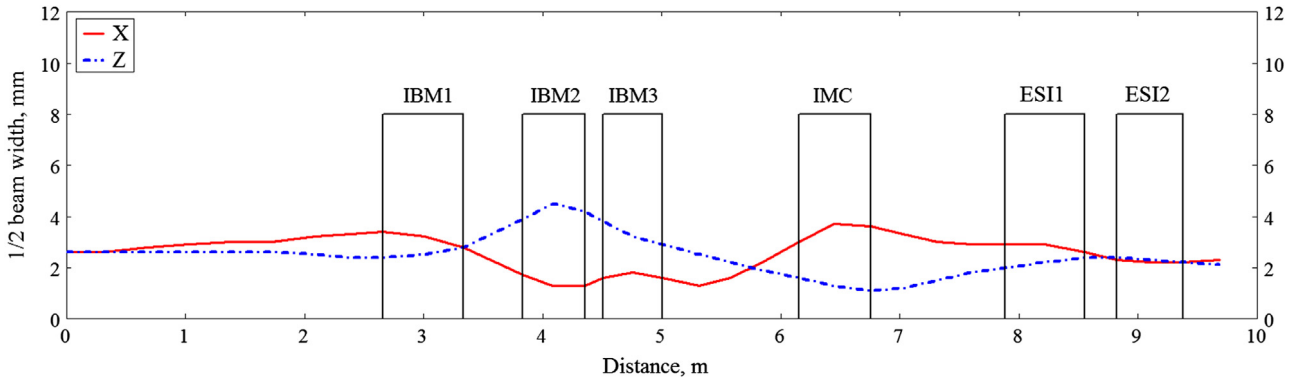

Fig. 14. Beam envelopes along the injection line.

orbits to 15 Gs, the return yoke of the magnet has an enforced thickness of 90 mm. The length of the magnet is 164 cm, and its weight is 900 kg.

5. Beam dynamics simulation

Digital simulation of the beam transmission and acceleration was performed beginning with the interface point between the K280 and the K1600 and ending with the final radius of the particle orbits in the K1600 using the 3D ray-tracing program SNOP [18]. For the best efficiency of injection, the injected beam should be of very good quality at the K1600 valley entrance. The following parameters of the beam were chosen for the dynamics analysis: transverse emittances 2 π mm mrad, transverse size 5 mm, the Twiss parameter $\alpha \approx 0$, and the RF phase range in the beam 10° RF. The angular spread in the beam is below ±1 mrad. The transverse emittances of the beam, which is extracted from the K280, can reach 10–20 π mm mrad. But since the expected K280 output beam intensity is about 600–800 nA, a suitable collimator system permits reaching the required transverse quality of the beam at the K1600 entrance. Given sufficiently effective beam transmission through the K1600, the final intensity of the beam, exiting the K1600 can reach the required 100–200 nA.

The distance from the entrance of the K1600 to the first K1600 injection bending magnet is ~2.5 m. There is no dedicated beam focusing elements in this region, but particles moving along curvilinear trajectories see nonuniform (either increasing or decreasing in space) magnetic field of the main cyclotron itself. This leads to alternative focusing of the particles, which explains not only small angular deviation but also low transverse size of the beam at the entrance of the first injection magnet. At the initial orbits in the K1600 the distance between the neighboring orbits is ~5 mm. Simulations show that in the injection process the transverse deviation of the particles from the reference ion trajectory is less than ±5 mm (Fig. 14). The size of the beam passing through the ESIs is quite moderate (±2 mm), leading to the beam losses on the septums of the inflectors less than ~15%.

There are practically no beam losses downstream the injection zone up to the final radius of the K1600. The turn separation due to the energy gain is ~1.5 mm at the final radius. Since the radial betatron frequency is far from unity there, the introduction of the first magnetic harmonic does not permit a sufficient increase in this turn separation. In this case, introduction of suitable off-centering of the particle orbits at the injection really helps. For example, it is sufficient to induce a 6-mm radial amplitude at the injection to get ~5 mm turn separation at the ESD entrance. It is worthwhile to notice that the off-centering of the initial beam orbits is highly dependent on the existing first magnetic field harmonic amplitude due to the fringe field of the injection system elements. In the preliminary assessment of the beam dynamics the fringe fields of the injection system were neglected in the analysis until future optimization of the injection system structure. So, the orbits off-centering was provided by introducing the artificial first harmonic amplitude of 10–12 Gs. Since at the final K1600 radius the radial size of the accelerated bunch is ~12 mm, neighboring orbits overlap, which leads to a multi-turn extraction with the efficiency of ~75%. The horizontal and axial beam emittances of the extracted beam are 20 and 1.4 π mm mrad at an observation point outside of the cyclotron. The energy spread in the beam is about ±1.2 MeV/u with the average energy of ~405 MeV/u. The horizontal and axial sizes of the beam are ±6 mm and ±2 mm correspondingly. Since the output beam intensity are much higher than required for the final user, the corresponding handling system outside the accelerator can ensure required transverse quality of the beam. Besides, the single-turn extraction mode with the more than 90% efficiency is possible by selecting a 5–6 RF degree bunch at the injection to the K1600. Obviously, the beam parameters are much better in this case to meet the existing requirements.

6. Summary

Initial design study was carried out to show that a coupled superconducting cyclotron complex is a serious candidate for medical ion applications. The facility under consideration is more compact than the similar-purpose synchrotron and simpler to operate. The cyclotron elements specified in the current version of the design are realistically achievable. Obviously, the obtained results are of very preliminary nature and further work on the project is needed. For example, the RF system design, cryogenic system, ponderomotive forces in both cyclotrons require special consideration. Also, study of the fringe fields in the cyclotrons, formulation of tolerances on these fields in various regions outside the facility, and methods of their shielding are a separate important task to fulfill. The most difficult problem in this sense is injection to the K1600 and extraction from this accelerator under appropriate suppression of the fringe fields in the inner orbits in the vicinity of the structure elements of these systems. The beam lines from the ion source to the K280 and at injection to K1600 also require additional consideration.

References

[1] V.L. Smirnov, S.B. Vorozhtsov, Modern compact accelerators of cyclotron type for medical applications, Phys. Part. Nucl. 47 (5) (2016) 863–883.
[2] J.M. Schippers, et al., A novel design of a cyclotron based accelerator system for multi-ions therapy, in: Proc. of the Int. Conf. on Heavy Ion Accelerator Technology (HIAT'09), Venice, Italy, 2009, pp. 74–78.
[3] D. Ondreka, U. Weinrich, The Heidelberg Ion Therapy (HIT) accelerator coming into operation, in: Proc. of EPAC'08, Genoa, Italy, 2008, p. 979.
[4] S. Rossi, Eur. Phys. J. Plus 126 (8) (2011) 78.
[5] Guoqing Xiao, Status of heavy-ion therapy at institute of modern physics chinese academy of sciences, in: Proc. of Annual Conf. Of The Particle Therapy Co Operative Group, Shanghai, China, 2014.
[6] V. Smirnov, S. Vorozhtsov, A coupled cyclotron solution for carbon ions acceleration, in: Proc. of the 21th Int. Conf. Cyclotrons'16, Zurich, Switzerland, 2016, pp. 270–273.

[7] V. Smirnov, S. Vorozhtsov, A cyclotron complex for acceleration of carbon ions, in: Proc. of the XXV Russian Accelerator Conference (RuPAC'2016), Peterhof, St. Petersburg, Russia, 2016, pp. 467-470.
[8] L.A.C. Piazza, SCENT 300 Project, Status Review, XXXVIIECPM –Groningen, 2009.
[9] A.E. Geisler, et al., Commissioning of the ACCEL 250 MeV proton cyclotron, in: Proc. of the 18th Int. Conf. Cyclotrons'07, Giardini Naxos, Italy, Oct. 2007, pp. 9–14.
[10] B. Qin, et al., Design study of a 250 MeV superconducting isochronous cyclotron for proton therapy, in: Proc. of SAP2014, Lanzhou, China.
[11] T. Zhang, et al., Developments for 230 MeV superconducting cyclotrons for proton therapy and proton irradiation, Nucl. Instrum. Methods Phys. Res. (2016).
[12] G. Karamysheva, et al., Present status of the SC202 superconducting cyclotron for hadron therapy development, in: Proc. of IPAC'17, Copenhagen, Denmark, 2017.
[13] http://www.pantechnik.com/#!sources/vstc2=supernanogan.
[14] Y. Jongen, et al., IBA-JINR 400 MeV/u superconducting cyclotron for hadron therapy, in: Proc. of the 19th Int. Conf. Cyclotrons'10, Lanzhou, China, 2010, pp. 404–409.
[15] V. Smirnov, S. Vorozhtsov, Magnetic system of a superconducting separated-sector cyclotron for hadron therapy, Phys. Part. Nucl. Lett. 14 (4) (2017) 658–668.
[16] M.M. Gordon, Computation of closed orbits and basic focusing properties for sector focused cyclotrons and the design of "Cyclops", Part. Accelerators 16 (1984) 39–62.
[17] N. Sakamoto, M. Fujimaki, A. Goto, M. Kase, O. Kamigaito, R. Koyama, K. Suda, K. Yamada, S. Yokouchi, RF system for heavy ion cyclotrons at RIKEN RIBF, in: Proc. of the Int. Conf. on Heavy Ion Accelerator Technology (HIAT'09), Venice, Italy, 2009, pp. 69–73.
[18] V.L. Smirnov, S.B. Vorozhtsov, SNOP – beam dynamics analysis code for compact cyclotrons, in: Proc. of the XXIII Russian Accelerator Conference, RuPAC'2012, St. Petersburg, Russia, 2012, pp. 325–327.